Microscopic Structure of *DX* Centers in $Cd_{0.8}Zn_{0.2}Te$:Cl

Y. Y. Shan and K. G. Lynn
Department of Physics, Washington State University, Pullman, Washington 99164

Cs. Szeles
eV Products, a division of II-VI, Inc., Saxonburg, Pennsylvania 16056

P. Asoka-Kumar*
Department of Physics, Brookhaven National Laboratory, Upton, New York 11973

T. Thio and J. W. Bennett
NEC Research Institute, Princeton, New Jersey 08540

C. B. Beling and S. Fung
Department of Physics, The University of Hong Kong, Hong Kong

P. Becla
Department of Materials Science and Engineering, Massachusetts Institute of Technology, Massachusetts 02139
(Received 16 June 1997)

Photoexcitation of chlorine *DX* centers induces a transition of the Cl atoms to the shallow-donor state and persistent photoconductivity at low temperature in $Cd_{0.8}Zn_{0.2}Te$:Cl. The relaxation of the substitutional Cl atoms to the *DX* state at 140 K is coincident with a decrease of the positron lineshape parameter and an increase of annihilation with high-momentum core electrons. The results indicate positron trapping and annihilation at *DX* centers and at chlorine *A* centers. The data support the bond breaking model of the *DX* centers and the outward relaxation of the Cl and Cd(Zn) atoms along the [111] direction. The thermal barrier for the shallow-deep transition was found to be 0.44 eV. [S0031-9007(97)04418-9]

PACS numbers: 78.70.Bj, 61.72.Ji

The microstructure and electrical properties of *DX* centers have been successfully described by the relaxation of donor atoms from the substitutional lattice position in III-V compounds [1–5]. The resulting *DX* state is a negative-*U* center that is doubly occupied and negatively charged in its ground state. The deep-acceptor state (DX^-) can be converted to the shallow-donor state (d^+) by photoexcitation at low temperature. The d^+ state is metastable and exhibits persistent photoconductivity (PPC). At higher temperatures thermal excitation is sufficient to overcome the barrier and the substitutional-donor atom relaxes to the *DX* state. The lattice-relaxation model was promoted for *DX* centers in II-VI compounds as well [6]. The theoretical model suggested three possible configurations for chlorine *DX* centers in $Cd_{1-x}Zn_xTe$ [6].

In this Letter, we report the observation of the atomic-structure change related to the shallow-deep transition of chlorine *DX* centers in $Cd_{0.8}Zn_{0.2}Te$:Cl using positron annihilation spectroscopy (PAS) and thermoelectric (TE) transport measurements. To identify the *DX* centers and study the shallow-deep transition of the Cl atom temperature-dependent TE conductivity measurements were carried out. The two-detector coincidence spectroscopy of positron-annihilation radiation was used to determine the microstructure of the *DX* centers. The results suggest that Cl *DX* centers in $Cd_{0.8}Zn_{0.2}Te$:Cl involve a breaking of the Cd(Zn)-Cl bond along the [111] direction and an outward relaxation of the Cd(Zn) and Cl atoms.

The $Cd_{0.8}Zn_{0.2}Te$:Cl crystal studied in these experiments was grown by the vertical Bridgman technique [7]. The sample was annealed in Cd vapor at 0.02 atm at 600 °C for 5 days to decrease the concentration of acceptors such as Cd(Zn) vacancies and Cl *A* centers (Cd vacancy-Cl pairs). The electrodes were prepared using an In-Sn eutectic alloy. The TE transport measurements were performed using an optical cryostat operating in the 9–370 K temperature range [8]. In TE current experiments the driving force for carrier transport is provided by the temperature gradient in the sample. Since both charge carriers diffuse in the same direction the opposite sign of the thermoelectric power for electrons and holes produces TE currents of the opposite sign and allows the identification of the mobile charge carriers. The photoexcitation of the sample was performed using $h\nu = 1.51$ eV photons from a Xe lamp coupled to an optical monochromator for the TE current experiments and $h\nu = 1.33$ eV photons from a light-emitting diode for the PAS experiments. The TE current measurements showed *n* type conductivity and a saturated electron density of 6×10^{16} cm^{-3} after photoexcitation at 10 K consistent with earlier Hall-effect measurements [5].

The PAS [9,10] experiments were carried out using a variable-energy monoenergetic positron beam. The momentum distribution of the electrons annihilating with positrons was determined by measuring the Doppler broadening of the 511 keV annihilation γ line using a high-resolution γ-spectroscopy system. To monitor the change in the momentum distribution due to the shallow-deep transition of *DX* centers the line-shape parameter (S) was defined as the ratio of counts in the central region (511 ± 0.83 keV) of the photopeak to the total counts in the peak. The reproducibility of the S parameter in this digitally stabilized system was better than 0.0004. The S parameter measures mostly the contribution of the low-momentum valence electrons. The high-momentum components in the momentum distribution originate mostly from the core electrons at the annihilation site and can be used to extract information on the chemical composition of defects [11]. Here we used the two-detector coincidence spectroscopy to measure the high-momentum components in the momentum distribution [12].

Figure 1 shows the TE photoconductivity of the sample below and above the transition temperature (130–150 K) of *DX* centers [5]. For 10 and 90 K the photocurrents persisted after the photoexcitation terminated. At 170 K the photocurrent rapidly decays at the end of photoexcitation. The sign of the TE current shows that the free carriers generated by the photoexcitation are electrons consistent with the transition of Cl atoms to the shallow-donor state. Figure 2 shows the TE current vs temperature after photoexcitation with 1.51 eV photons at 10 K. The TE current increases with temperature and reaches a maximum at about 130 K. Above 140 K the current drops 2 orders of magnitude. The peak at 130 K is absent if no photoexcitation was performed at low temperature. The temperature dependence of the TE conductivity is reversible below 100 K. The Arrhenius plot of the TE current in this region gives an activation energy of 8 meV in agreement with the temperature dependence of the electron mobility and hopping transport through localized states at the conduction-band edge [5]. The PPC below 100 K and the decay of the TE current above 130 K indicates that a thermal barrier exists for the capture of electrons and the return of substitutional Cl donors to the stable state. Above 190 K the electron current increases with an activation energy of about 0.22 eV due to the thermal ionization of a deep-acceptor state.

The results are characteristic for *DX* centers in III-V and II-VI compounds [1–5]. We associate the observations with the photoinduced transition of the chlorine *DX* centers to the shallow-donor state (d^+) of substitutional Cl atoms at Te sites at low temperature and the thermally activated relaxation of the Cl_{Te} atom to the *DX* state in the 130–150 K temperature range. The electronic level of the *DX* state is deep in the band gap and its thermal ionization occurs only at higher temperature.

Figure 3 shows the S parameter as a function of the positron incident energy (S-E) before and after photoexcitation. After saturation illumination at 50 K the bulk S value increased to 1.0028. Like the PPC, this increase is metastable and can be annealed out at 130–150 K. Figure 4 shows the S parameter as a function of isochronal annealing after photoexcitation at 50 K. The sample was cooled to 50 K after each annealing to eliminate the effects of the temperature-dependent positron annihilation and transport parameters. The higher S parameter induced by photoexcitation was stable up to 130 K and the lower S was recovered above 150 K. No annealing effect was observed without the low-temperature photoexcitation.

The difference between the surface and bulk S parameters allows the measurement of the positron diffusion length (L_+) by fitting a diffusion-annihilation equation to the S-E data [13]. The very short $L_+ = 270 \pm 20$ Å indicates that virtually no positron diffusion takes place in the material and the implanted positrons are rapidly trapped at lattice defects. In addition, L_+ is independent of temperature in the 50–150 range and does not change with photoexcitation. In Cl doped $Cd_{1-x}Zn_xTe$ crystals chlorine *A* centers, i.e., Cd(Zn) vacancy-Cl atom

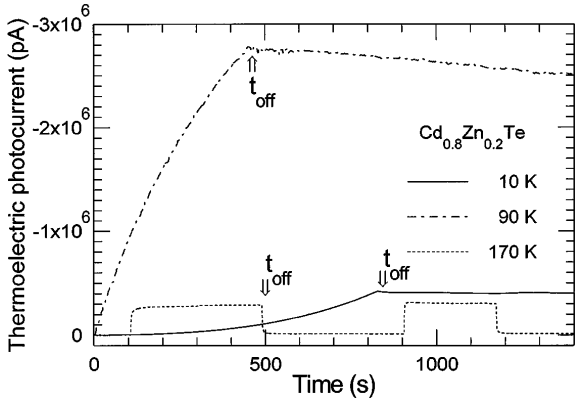

FIG. 1. Evolution of the thermoelectric photocurrent (zero bias) for photoexcitation by 1.51 eV photons at 10, 90, and 170 K, respectively. t_{off} indicates the end of illumination. PPC was observed at 10 and 90 K.

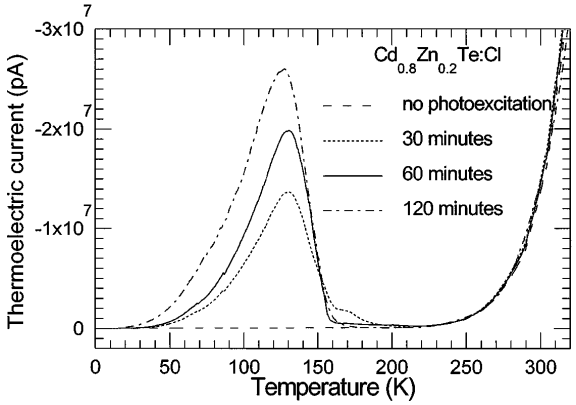

FIG. 2. Temperature dependence of the thermoelectric current for photoexcitation by 1.51 eV photons at 10 K for 30, 60, and 120 min. The TE current saturates for 120 min illumination. The experiments were performed at a 0.42 K/s heating rate.

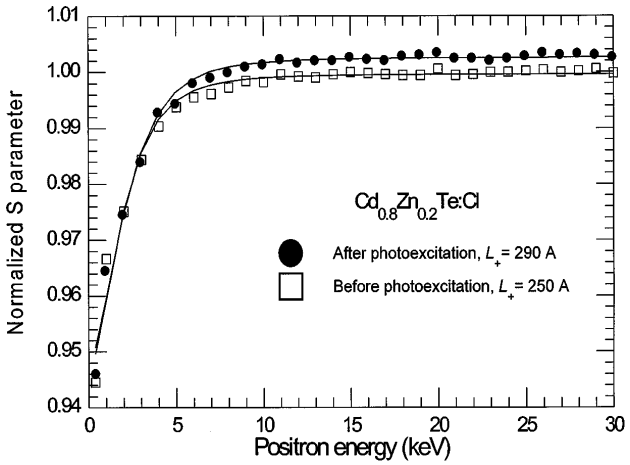

FIG. 3. The normalized S parameter as a function of the incident positron energy at 50 K. The S parameter was normalized to the bulk S value before photoexcitation.

pairs (V_{Cd}-Cl_{Te}) are formed in large concentration [14]. The A centers that have an acceptor level 0.12–0.14 eV above the valence band maximum [15] are negatively charged in n type material and are effective positron traps. Trapping of positrons at the Cd(Zn) vacancy of the Cl A center explains the higher S parameter when the DX^- centers are converted to the d^+ state. Although the A-center concentration was considerably reduced by annealing the sample in Cd vapors the residual acceptor concentration is significant ($\sim 10^{15}$ cm^{-3}) [4] and can account for the observed positron trapping. In addition, positron trapping at extended defects and residual impurities can also contribute to the short L_+ [10].

The strong correlation between the photoexcitation and temperature dependence of the S parameter and the TE current indicates that the positrons are sensitive to the transition of the Cl atoms between the DX^- and the shallow-donor state. The higher S after photoexcitation is characteristic for the situation when most of the Cl atoms are in the d^+ state while the lower S value reflects the condition when a high fraction of the Cl atoms is in the DX configuration.

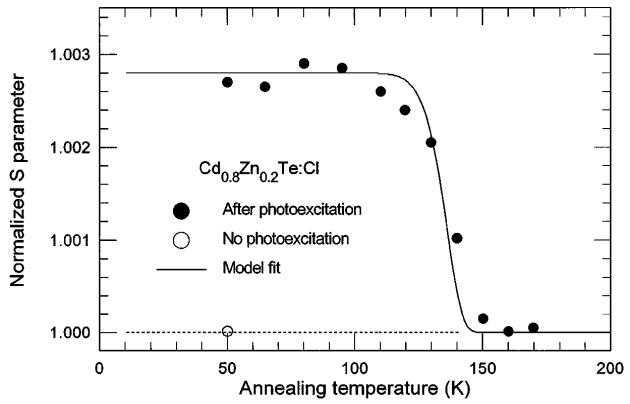

FIG. 4. The S parameter as a function of the annealing temperature. The isochronal annealing was performed for 15 min. The positron incident energy was fixed at 15 keV to ensure implantation to the bulk.

Trapping of positrons at the negatively charged DX^- centers explains the sensitivity of positrons to the $d^+ \leftrightarrow DX^-$ transition of the Cl atoms. The difference in the S parameter upon the $d^+ \leftrightarrow DX^-$ transition reflects the different local environment experienced by the positrons trapped at A centers and DX^- centers. After saturation photoexcitation the concentration of DX centers is negligible and the positrons are trapped at Cl A centers. The trapped state is characterized by a higher S value due to the low overlap of the positron wave function with the high-momentum core electrons at the Cd(Zn) vacancy. The short positron diffusion length indicates that virtually no delocalized positrons contribute to the S parameter. Above 150 K positrons are trapped at the DX^- centers and the lower S value reflects the atomic configuration and chemical environment of the DX centers.

The S as a function of annealing temperature is given by

$$S(T) = f_1(T)S_1 + [1 - f_1(T)]S_2\,, \qquad (1)$$

where $f_1(t) = \gamma_2/(\gamma_1 + \gamma_2) + [1 - \gamma_2/(\gamma_1 + \gamma_2)] \exp \times [-(\gamma_1 + \gamma_2)t]$ is the fraction of Cl atoms in the metastable d^+ state. S_1 and S_2 are the S parameters after and before photoexcitation. $\gamma_1 = \gamma_0 \exp(-E_1/kT)$, and $\gamma_2 = \gamma_0 \exp(-E_2/kT)$ are the thermal transition rates from the d^+ state to the DX^- state and back, respectively. $\gamma_0 \sim 10^{13}$ s^{-1} is the attempt frequency, E_1 is the thermal recombination barrier (i.e., transition from the d^+ state to the DX state), and E_2 is the thermal emission barrier (i.e., the transition from the DX state to the d^+ state). Since $E_2 > E_1$ the transition in Figs. 2 and 4 is governed by the thermal recombination barrier (E_1). By fitting Eq. (1) to the S parameter data in Fig. 4 the recombination barrier of $E_1 = 0.44 \pm 0.04$ eV was obtained.

In order to determine the atomic structure of the DX centers the two-detector coincidence spectroscopy was employed [11,12]. The technique measures the momentum distribution of core electrons of the first-nearest-neighbor atoms at the defect where the positron is localized. Since the core electrons retain their atomic character even when the atoms form a solid the high-momentum components of the momentum distribution reflect the chemical composition of the defects [11]. Figure 5 shows the change in positron annihilation with the high-momentum core electrons upon photoexcitation and annealing at 140 K. The data indicate higher contribution from high-momentum ($P_L > 28 \times 10^{-3} m_0 c$) core electrons when the positrons are trapped at DX centers and a significantly lower contribution when they are trapped at Cd(Zn) vacancies of the chlorine A centers. Recently Park and Chadi [6] proposed three alternative configurations for Cl DX centers in $Cd_{1-x}Zn_xTe$:Cl crystals (Fig. 6). One (DX_1) configuration represents the breaking of a Cd(Zn)-Cl bond and the outward relaxation of the Cd(Zn) and Cl_{Te} atoms along the [111] direction. This configuration creates a free volume

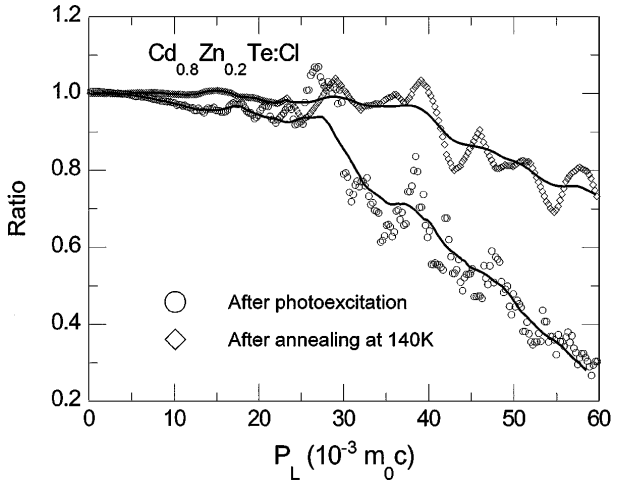

FIG. 5. Momentum-distribution spectra upon 1.33 eV photoexcitation at 50 K, and annealed at 140 K. The spectra are normalized to the spectrum without photoexcitation. The lines are guides for the eye. The *DX* state is not fully recovered at 140 K.

along the broken Cd(Zn)-Cl bond. In the two other (DX_2 and DX_3) configurations the relaxation of the Cd(Zn) and Cl atoms creates a compression of the Cd(Zn)-Cl bond. The PAS data presented here are consistent with positron localization at the DX_1 center and the smaller free volume available for positron localization at the center than at the *A* centers. This results in a larger overlap of the localized positron wave function with the first-nearest-neighbor core electrons, particularly with the core electrons of the relaxed Cd(Zn) atom. The trapping at the DX_1 center fully explains the observed lower *S* parameter and the higher high-momentum core electron contributions compared to the condition when the positrons are trapped at *A* centers.

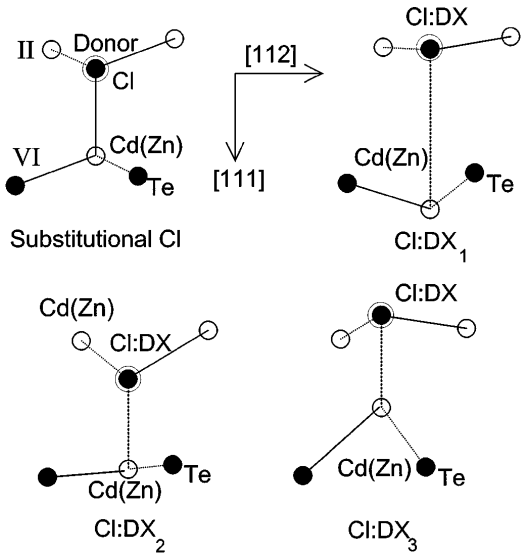

FIG. 6. The proposed configurations of Cl *DX* centers on a (110) plane in $Cd_{0.8}Zn_{0.2}Te$:Cl [6]. Dotted lines are bonds not in the (110) plane, and dashed lines are broken or compressed bonds.

In conclusion, positron annihilation spectroscopy and thermoelectric current measurements have been carried out to study the microscopic structure and shallow-deep transition of chlorine *DX* centers in $Cd_{0.8}Zn_{0.2}Te$:Cl. The transition is coincident with a sharp decrease of the positron line-shape parameter (*S*) and a significant increase of positron annihilation with high-momentum core electrons. The results indicate positron trapping and annihilation at chlorine *A* centers after photoexcitation and at *DX* centers after annealing. Among the three *DX* geometries proposed for chlorine *DX* centers in $Cd_{1-x}Zn_xTe$[6] [6] the results support the bond-breaking geometry and the outward relaxation of the Cl and Cd(Zn) atoms along the [111] direction (DX_1). The thermal barrier for the shallow-deep relaxation was estimated to be 0.44 eV.

The BNL part of this work was supported by the Department of Energy under Contract No. DE-AC02-76CH00016.

*Present address: Lawrence Livermore National Laboratory, Livermore, CA 94551.

[1] D. V. Lang, in *Deep Centers in Semiconductors*, edited by S. T. Pantelides (Gordon and Breach, New York, 1987).
[2] P. M. Mooney and T. N. Theis, Comments Condens. Matter Phys. **16**, 167 (1992).
[3] D. J. Chadi and K. J. Chang, Phys. Rev. Lett. **61**, 873 (1988).
[4] K. Khachaturyan, M. Kaminska, E. R. Weber, P. Bech, and R. A. Street, Phys. Rev. B **40**, 6304 (1989).
[5] J. W. Bennett, T. Thio, S. E. Kabakoff, D. J. Chadi, R. A. Linke, and P. Becla, J. Appl. Phys. **78**, 582 (1995); T. Thio, J. W. Bennett, and P. Becla, Phys. Rev. B **54**, 1754 (1996).
[6] C. H. Park and D. J. Chadi, Appl. Phys. Lett. **66**, 3127 (1995).
[7] P. Becla, D. Kaiser, N. C. Giles, Y. Lansari, and J. F. Schetzina, J. Appl. Phys. **62**, 1352 (1987).
[8] Cs. Szeles, Y. Y. Shan, K. G. Lynn, and E. E. Eissler, Nucl. Instrum. Methods Phys. Res., Sect. A **380**, 148 (1996).
[9] P. J. Schultz and K. G. Lynn, Rev. Mod. Phys. **60**, 701 (1988).
[10] K. Saarinen, P. Hautojarvi, and C. Corbel, *Identification of Defects in Semiconductors*, edited by M. Stavola (Academic Press, New York, 1997).
[11] P. Asoka-Kumar, M. Alatalo, V. J. Ghosh, A. C. Kruseman, B. Nielsen, and K. G. Lynn, Phys. Rev. Lett. **77**, 2097 (1996).
[12] K. G. Lynn, J. E. Dickman, W. L. Brown, M. F. Robbins, and E. Bonderup, Phys. Rev. B **20**, 3566 (1979).
[13] A. van Veen, H. Schut, J. de Vries, R. A. Hakvoort, and M. R. Ijpma, in *Slow Positron Beams for Solids and Surfaces*, edited by P. J. Schultz, G. R. Massoumi, and P. J. Simpson (AIP, New York, 1990), p. 171.
[14] M. Hage-Ali and P. Sieffert, Nucl. Instrum. Methods Phys. Res., Sect. A **322**, 313 (1992).
[15] D. M. Hoffman, P. Omling, H. C. Grimmeiss, B. K. Meyer, K. W. Benz, and D. Sinerius, Phys. Rev. B **45**, 6247 (1992).